International Journal of Thermodynamics (IJoT)
ISSN 1301-9724 / e-ISSN 2146-1511
https://dergipark.org.tr/en/pub/ijot

Vol. 26 (No. 1), pp. 018-024, 2023
doi: 10.5541/ijot.1157497
Published online: March 1, 2023

Research Article

Thermodynamic Studies on $Sr_5Nb_4O_{15}$

[1]*P. Samui, [2]S.M. Bhojane, [2]B.M. Singh, [2]S.K. Rakshit

[1,2] Product Development Division, BARC, Trombay, Mumbai, India- 400 085
[1,2] Homi Bhabha National Institute, BARC, Mumbai-85
E-mail: [1]* pradeepsamui@gmail.com

Received 8 August 2022, Revised 9 November 2022, Accepted 16 December 2022

Abstract

The SrO–Nb_2O_5 system, especially $Sr_5Nb_4O_{15}$ compound is of interest for their use as an electroceramics. In this work, $Sr_5Nb_4O_{15}$ compound was synthesized by solid-state reaction and characterised by XRD. Thermodynamic properties like heat capacity, enthalpy of formation and Gibbs energy of formation of $Sr_5Nb_4O_{15}$ have been measured. The standard molar enthalpy of formation of $Sr_5Nb_4O_{15}$(s) was determined using an oxide melt solution high temperature calorimeter. Based on these experimental data, a self-consistent thermodynamic function of this compound was also generated. This thermodynamic data is essential for the optimization of synthesis conditions for materials and for the evaluation of their stability under appropriate technological operating conditions.

Keywords: *Heat capacity; dsc; high temperature calorimeter; enthalpy of formation; niobates.*

1. Introduction

Strontium niobates in the binary system SrO–Nb_2O_5 are potential multifunctional materials with cation-deficient perovskite structure. They have high dielectric constant, less dielectric loss, and low temperature dependence of dielectric constant. They are promising materials for microwave ceramics [1-3]. They are also investigated as valuable crystal host for luminescent lanthanide ions [4]. $Sr_5Nb_4O_{15}$ is mainly interesting for their promising photocatalytic activity [5]. Furthermore, in the nuclear industry, ternary oxides of strontium and niobium may form as fission product compounds in an operating nuclear reactor with oxide fuels under certain oxygen potential. Evaluations of thermodynamic stability of these ternary oxides are therefore important for assessment of fission product interactions. $Sr_5Nb_4O_{15}$(s) is highest melting compound in the SrO-Nb_2O_5 system. Whiston and Smith have first reported the existence of $Sr_5Nb_4O_{15}$ compound which is a iso-structural with the tantalum analogue [6]. Earlier, crystal structure analysis of the $Sr_5Nb_4O_{15}$ compound was performed by Weiden et al. [7]. Recently, in-depth crystal structure analysis on $Sr_5Nb_4O_{15}$ point to that it crystallizes in the trigonal P-3c1 space group, which is considered to be a subsection of hexagonal structure [8]. The structure contents three inequivalent Sr^{2+} sites, two inequivalent Nb^{5+} sites and three inequivalent O^{2-} sites [8]. Phase relations in the binary system SrO–Nb_2O_5 were investigated by Carruthers and Grasso [9] and more recently by [10]. A thermodynamic assessment of the SrO–Nb_2O_5 system was accomplished by Yang et al. [11]. Thermodynamic functions of oxides reported in SrO–Nb_2O_5 system were assessed using Calphad technique. Leitner et al [12] measured heat capacities (20-350 K) and enthalpy increments (670-1370 K) of strontium niobates. The standard molar entropies at 298 K have been reported from low temperature heat capacity data. There is no experimentally determined heat capacity of this compound from 350-670 K. The Gibbs energy of formation and enthalpy of formation of the compound is not available in literature. Moreover, thermodynamic data of these oxides are also of relevance to compute phase diagram and phase stability of multicomponent systems. Hence, in the present study, $Sr_5Nb_4O_{15}$(s) was prepared and characterized first. Then heat capacity, Gibbs energy of formation and enthalpy of formation of the compound was determined employing differential scanning calorimetry, Knudsen effusion technique and high temperature oxide melt solution calorimeter, respectively. The thermodynamic table of this compound was also evaluated using heat capacity data.

2. Experimental Procedure

2.1. Synthesis of Compounds and Characterization

$Sr_5Nb_4O_{15}$(s) powder sample was prepared using conventional solid state reaction route using $SrCO_3$ (Alfa Aesar, mass fraction 0.9995) and Nb_2O_5 (Alfa Aesar, mass fraction 0.999). Prior to mixing, $SrCO_3$(s) and Nb_2O_5(s) were first dried under the flow of high purity Ar(g) at 873 K for 8 h and then cooled overnight under continuous flow of Ar(g). Stoichiometric amount of dried carbonate and Nb_2O_5 were properly mixed using an agate mortar and pestle and made into pellets. The pellet was then heated at 1000 K in a platinum boat for a period of 120 h with three intermediate grindings. Finally, the pellets were powdered and stored inside desiccator. Phase formation and lattice parameters of $Sr_5Nb_4O_{15}$(s) were determined using a Miniflex 600 X-ray diffractometer (Model: Rigaku, Japan) with graphite monochromatized Cu $K\alpha_1$ radiation (λ = 0.15406 nm).

*Corresponding Author

2.2 Knudsen Effusion Quadruples Mass Spectrometry (KEQMS)

In this study, an indigenously developed Residual Gas Analyzer (RGA) (Model: Hiden HAL/3F 501, UK) based on quadruple mass spectrometer connected to a Knudsen effusion system was used for measurement of equilibrium partial pressures of permanent gases. The details of the experimental setup have been described by Rakshit et al. [13]. For the sake of clarity, schematic of KEQMS has been presented in Figure 1. The temperature near the Knudsen cell was measured using a pre-calibrated (ITS-90) chromel–alumel thermocouple. The Knudsen cell used was made of boron nitride (BN) with a knife edged orifice of diameter 0.8 mm at the centre of the upper lid. A Faraday cup detector is used to collect the ions generated which is proportional to ion intensity. The ion intensity of the i^{th} ion is related to partial pressure and is represented as:

$$p_i = K_{inst} \cdot (I_i^+ \cdot T)/(\sigma_i \cdot a_i) \quad (1)$$

Where, K_{inst} is the instrumental constant, I_i^+ is the measured ion current in ampere, T is the absolute temperature, σ_i is the electron impact cross-section and a_i is the isotopic abundance of the specific ion. Taking natural logarithm on both sides, the Eq. (1) can be written as:

$$\ln p_i = \ln K_{inst} + \ln(I_i^+ T) - \ln \sigma_i - \ln a_i \quad (2)$$

For permanent gaseous species such as CO_2^+ (m/e =44), the value of $\ln\sigma_i$ is - 45.52 at 30 eV [14]. The isotopic abundance of CO_2 is taken as 100% ($\ln a_i = 0$). Thus, Eq. (2) becomes

$$\ln\{p(CO_2/\text{atm})\} = \ln K_{\text{inst}} + \ln(I^+T) + 45.52 \quad (3)$$

For Knudsen effusion quadruple mass spectrometry (KEQMS) experiment, a phase mixture of {$Sr_5Nb_4O_{15}$ (s) + Nb_2O_5(s) + $SrCO_3$(s)} was prepared by homogenously mixing the individual compounds in their stoichiometric proportions under moisture free condition and made into pellet. The pellet was heated at 700 K and stored inside desiccators.

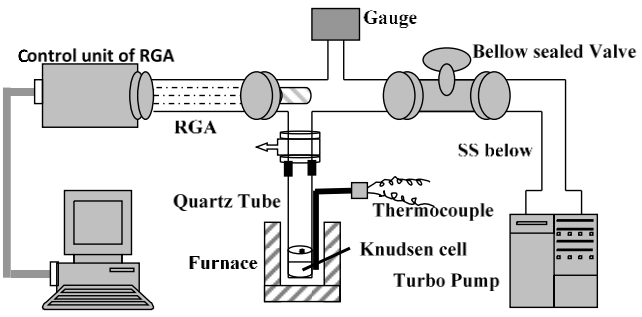

Figure 1. Schematic diagram of KEQMS setup.

2.3 Measurement of Heat Capacity using Differential Scanning Calorimeter

A standard three step method [15], blank-blank, blank-reference and blank-sample was followed for the measurement of the heat flow rate signal of base line, reference and sample, respectively. Heat capacity measurements of known amount of $Sr_5Nb_4O_{15}$(s) were carried out in a platinum crucible with lids using Labsys Evo1600 simultaneous thermal analyzer system (Setaram Instrumentation, France). The flow rate of 30 mL·min^{-1} of dry argon (purity, 99.9999%) and a heating rate of 5 K·min^{-1} with continuous scanning mode was maintained during all measurements. The phase transition temperature of standard reference materials e.g. In, Sn, Pb, Al and Ag under the scanning rate of 2, 5 and 10 K·min^{-1} was measured for the temperature calibration of the DSC. A temperature correction factor as a function of heating rate was plotted and the value corresponding to zero heating rate was obtained. The corrected temperature was used for the heat capacity measurement of the compound. NIST synthetic sapphire (SRM-720, mass fraction purity 0.9999) was used as reference material with known heat capacity values obtained from the literature [16]. The values of heat capacity of Zirconia (Alfa Aesar, USA, mass fraction 0.99978) were measured in the same temperature range to check the accuracy of the calorimeter which was found to be within ±2% compared to the literature values [16].

2.4 High Temperature Solution Calorimetry

Standard molar enthalpy of formation of $Sr_5Nb_4O_{15}$(s) was determined by measuring the enthalpy change for the dissolution of $Sr_5Nb_4O_{15}$(s) and its starting materials such as $SrCO_3$(s) and Nb_2O_5(s) in liquid {$PbO + B_2O_3$} solvent (in 2:1 molar ratio) at 966 K using Alexsys high temperature calorimeter (Setaram, France). The details of experimental set up and its working formulae has been reported in our earlier publication [17]. ~10g of {$PbO + B_2O_3$} solvent (in 2:1 molar ratio) is taken inside a platinum crucible for each experiment. Three consecutive addition of solute in the solvent were carried out to check the reliability of the experimental data. Calibration of the calorimeter was performed by adding small pieces of synthetic sapphire [NIST SRM-720] [18] from 298 K into platinum crucible, maintained at 966 K. The weight of the sample and synthetic sapphire [NIST SRM-720] was in the range 20-50 mg, respectively. The accuracy of the instrument obtained using enthalpy increment values of molybdenum (99.997% purity) and NBS standard synthetic sapphire (SRM 720) was found to be better than ±2%.

3. Result and discussion

3.1 Characterization

The purity of $Sr_5Nb_4O_{15}$(s) powder was established by using X-ray diffraction (XRD) analysis. The XRD pattern of the sample is shown in Figure 2 and are compared with that of diffraction line of compound given in the reference (JCPDS XRD file No. 00-048-0421) [19]. The compound crystallizes in the distorted hexagonal unit cell (*P3m*) with the cell parameters a = b = 5.6552(5) Å and c = 11.4557(8) Å. They are in good agreement with that of reported cell parameters such as a = b = 5.6576(6) Å and c = 11.4536(4) Å [20]. No diffraction line corresponding to starting material phases and other unwanted phases were found in the XRD pattern indicating pure form of compound.

3.2 Gibbs Energy of Formation of $Sr_5Nb_4O_{15}$(S) using KEQMS

The calibration of the mass spectrometer with Knudsen cell setup was carried out by measuring the ion intensities of CO_2^+ using the phase mixture of {$SrCO_3$(s) + SrO(s)} at 30 eV ionization energy and keeping the other ion optic parameters constant for all sets of measurements. These ion

intensities and the partial pressure values of the CO_2 from the literature were used for the calculation of K_{inst}. The following equilibrium reaction was established inside the Knudsen cell.

$$SrCO_3(s) = SrO(s) + CO_2(g) \quad (4)$$

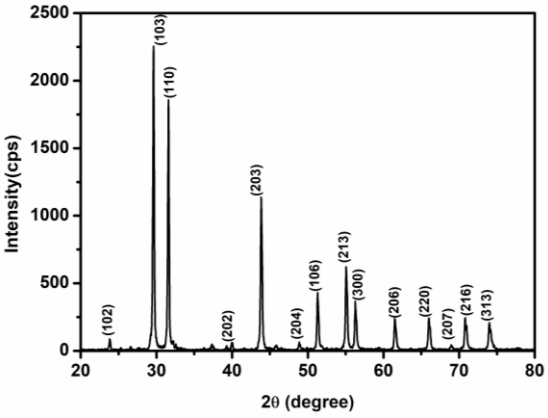

Figure 2. Powder XRD pattern of $Sr_5Nb_4O_{15}$*(s).*

The individual ion intensities of CO_2^+ peak over the equilibrium phase mixture were recorded at different temperatures. The ion intensities of several runs are least square fitted as a function of temperature and is expressed as:

$$\ln\{I^+(CO_2).T\} = -29426\ (\pm 494)\ /\ (T\ /\ \mathrm{K}) + 13.5\ (\pm 0.54)\quad (840 \le T/\mathrm{K} \le 950) \quad (5)$$

Values of instrument constant was determined by using Eq. (3) and values of partial pressure of CO_2(g) from literature [16] and experimentally determined ion intensity of CO_2(g) over the phase mixture {$SrCO_3$(s)+SrO(s)}. The calculated instrumental constant (K_{inst}) as a function of temperature is represented as:

$$\ln K_{inst}\ (\pm 0.04) = -39.2 + 633/(T/K) \quad (840 < T/\mathrm{K} < 950) \quad (6)$$

Ion intensity of CO_2^+ over the phase mixture of {$CaCO_3$(s) + CaO(s)} was also measured to check the accuracy of the measurements using the same experimental setup (Figure 1) after determining the partial pressures as a function of temperature. The corresponding equilibrium reaction was:

$$CaCO_3(s) = CaO(s) + CO_2(g) \quad (7)$$

The values of $\ln\{p(CO_2/\mathrm{atm})\}$ for Eq.(7) was calculated from Eq.(3) and using instrumental constant, Eq.(6) and other values for CO_2^+ ion. The corresponding expression is given as:

$$\ln\{p(CO_2/\mathrm{atm})\} = -21576\ (\pm 597)\ /\ (T/K) + 19.35\ (\pm 0.74)\quad (690 \le T/\mathrm{K} \le 865) \quad (8)$$

The enthalpy change related to reaction (7) at the average experimental temperature (T_{av} = 775 K) was calculated using Eq. (8) and found to be $\Delta_r H^\circ_m$ (775 K) = (179±5) kJ·mol^{-1}, which is in good agreement with that of literature (178.5 kJ·mol^{-1}) [16].

Prior to the actual experiment, the background signals were also monitored by heating the Knudsen chamber with empty Knudsen cell at different temperatures from ambient to 1160 K at a pressure level of 1×10^{-5} Pa. The background signals as a function of temperature are shown in Figure 3. It is evident from Figure 3 that the background signals corresponding to H_2^+, N_2^+, CO^+ and CO_2^+ do not change appreciably with change in temperature.

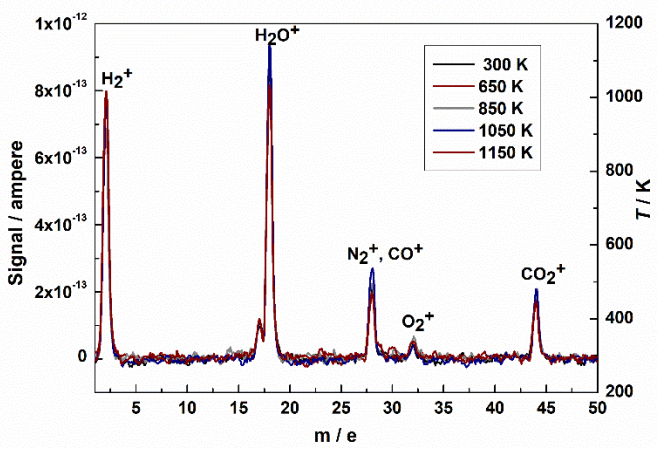

Figure 3: Background signal of KEQMS as a function of temperature.

During experiments, the actual signals were obtained by subtracting the ion intensities due to background. The ion intensities of CO_2^+ for {$Sr_5Nb_4O_{15}$(s) + 5$SrCO_3$(s) + 2Nb_2O_5(s)} phase mixture was measured at 30 eV ionization energy in the temperature range 870–1055 K. The values of ion intensity of CO_2 over the phase mixture were tabulated in Table 1.

Table 1. Ion intensities of CO_2 *peak over equilibrium phase mixture of {*$Sr_5Nb_4O_{15}$*(s) + 5*$SrCO_3$*(s) + 2*Nb_2O_5*(s)} as a function of temperature.*

T/K	I (CO_2^+)/A	*T*/K	I$^+$(CO_2^+)/A
871.6	4.00E-09	963.7	3.27E-08
887.6	5.49E-09	973.6	4.07E-08
903.2	7.92E-09	980.8	4.76E-08
919.0	1.22E-08	993.6	6.24E-08
934.2	1.66E-08	1013.6	9.73E-08
949.5	2.38E-08	1033.6	1.52E-07
951.6	2.58E-08	1054.7	2.34E-07

Partial pressures of CO_2, $p(CO_2)$, at different temperatures for three different runs were calculated using the measured ion intensities and the calibration constant from Eq. (6). Variation of $\ln p(CO_2)$ as a function of temperature is shown in Figure 4 which shows a linear trend and can be expressed as:

$$\ln\{p(CO_2/\mathrm{atm})\} = -20887\ (\pm 260)\ /\ (T/K) + 18.5\ (\pm 0.3)\quad (870 < T(\mathrm{K}) < 1055) \quad (9)$$

The following equilibrium reaction was established inside the Knudsen cell under experimental conditions,

$$5SrCO_3(s) + 2Nb_2O_5(s) = Sr_5Nb_4O_{15}\ (s) + 5CO_2(g) \quad (10)$$

The enthalpy change associated with the above reaction at the average temperature of the measurement was

estimated to be $\Delta_r H^0_m$ (962 K) = 868 kJ mol^{-1}. The standard molar Gibbs energy of reaction, $\Delta_r G^0_m(T)$, was calculated from Eq. (6) using the relation

$\Delta_r G^0_m(T)$ (kJ·mol^{-1})(±7)= (-RT ln p_{CO2})×0.001
= 868 + 0.8×T /K (870< T/K < 1055) (11)

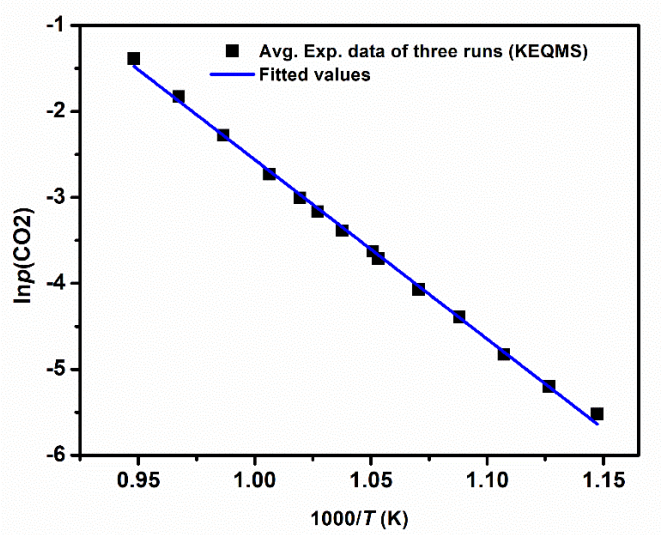

Figure 4: Variation of partial pressure of CO_2(g) as a function of temperature over ternary phase mixture {$Sr_5Nb_4O_{15}$ (s)+5$SrCO_3$(s)+2Nb_2O_5(s)}.

The standard molar Gibbs energies of formation of $Sr_5Nb_4O_{15}$ from the elements were calculated from Eq.(8) and the values of $\Delta_f G^0_m$ (T) for CO_2(g), $SrCO_3$(s) and Nb_2O_5(s) given in Table 2.

Table 2. Standard molar Gibbs energy of formation, $\Delta_f G^0_m(T)$ of different compounds [16,18].

Compound	$\Delta_f G^0_m(T)$(kJ.mol^{-1})
CO_2(g)	-394-0.0016×T
$SrCO_3$(s)	-1223+0.263×T
Nb_2O_5(s)	-1899+0.180×T

The corresponding expression

$\Delta_f G^0_m(Sr_5Nb_4O_{15}, s, T)$ (kJ.mol^{-1})(±8)
= -7075 + 1.3×T /K (870< T(K) < 1055) (12)

The enthalpy of formation of $Sr_5Nb_4O_{15}$(s) from their element at average temperature, 962 K, was -7075(±8) kJ·mol^{-1}.

3.3 Measurement of Heat Capacity

The molar heat capacities of $Sr_5Nb_4O_{15}$(s) were measured as a function of temperature from 300 K–1000 K and the values are presented in Table 3.

Variation of heat capacities of $Sr_5Nb_4O_{15}$(s) was plotted as a function of temperature and is shown in Figure 5. Low temperature heat capacity for this compound has been reported in literature [12] along with heat content of the compound from 670 K-1370 K. Authors have also assessed variation of $C_{p,\,m}$ function above room temperature by combining the data of heat capacity from DSC and the enthalpy increment from drop calorimetry. There is no direct measurement of high temperature heat capacity data reported in literature. The measured heat capacity data are compared with assessed C_p values in Figure 5.

Table 3. Variation of heat capacity of $Sr_5Nb_4O_{15}$(s) with Temperature. (T in K and $C_{p,m}$ in J·mol^{-1}·K^{-1}).

T	$C_{p,m}$	T	$C_{p,m}$
300.0	482.5	665.2	583.6
308.5	485.4	673.1	585.1
317.0	488.8	680.8	586.6
325.5	491.9	688.4	588.0
334.0	496.3	696.2	589.5
342.5	499.7	703.9	591.0
350.9	503.6	711.6	592.4
359.4	506.6	719.3	593.8
367.9	509.4	727.1	595.3
375.9	512.6	734.7	596.7
384.4	515.2	742.3	598.1
392.1	518.0	750.0	599.5
400.4	521.0	757.7	600.8
408.7	523.9	765.3	602.2
417.2	526.7	773.1	603.6
425.2	528.6	788.4	606.3
433.7	530.5	796.1	607.7
442.0	533.0	803.7	609.0
450.3	535.5	811.4	610.3
458.7	537.9	819.0	611.7
466.6	540.1	826.6	613.0
474.8	542.4	834.2	614.3
483.0	544.6	841.9	615.6
491.1	546.7	849.5	616.9
499.3	548.8	857.0	618.2
507.3	550.8	864.7	619.5
515.4	552.8	872.1	620.8
523.4	554.8	879.7	622.1
531.4	556.7	887.2	622.6
539.5	558.6	894.8	623.1
547.4	560.4	902.2	624.4
555.5	562.3	909.7	625.6
563.5	563.3	917.4	626.1
571.3	565.0	924.8	627.4
579.1	566.7	932.4	627.9
587.0	568.4	939.9	629.7
594.9	569.4	947.3	630.9
602.8	571.8	955.0	632.1
610.6	573.4	962.4	633.3
618.5	575.0	969.9	635.3
626.3	576.6	977.3	636.3
634.1	578.2	984.9	636.9
642.1	579.1	992.3	638.1
649.6	580.6	999.8	638.6
657.4	582.1	1007.3	639.1

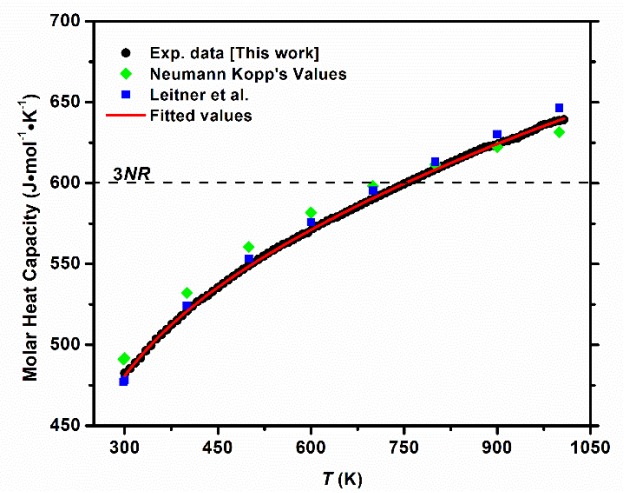

Figure 5: Variation of heat capacity with Temperature of $Sr_5Nb_4O_{15}$ (s) *compound*

The heat capacity data obtained in this study using DSC, is in good agreement with that of estimated one from Neumann Kopp's rule (NKR). The individual values of heat capacities were least square fitted as a function of temperature and the best fit is represented as

$$C^{o}_{p,\,m}\ (J\cdot mol^{-1}\cdot K^{-1}) = (501.3\pm1.3)+(0.1438\pm0.0014)\times(T/K)-(5928082\pm116602)/(T/K)^2\ (300 \le T/K \le 1000) \quad (13)$$

The heat capacity values of SrO and Nb_2O_5 for Neumann Kopp's rule (NKR) estimation are taken from the literature [16]. The estimated values of heat capacity using NKR are plotted in Figure 5. It can be seen that the heat capacity values obtained from DSC is slightly lower than the values calculated using NKR up to 900 K. Beyond 900 K, the DSC values is slightly higher than NKR values. According to Dulong Petit Law, the 3NR values for $Sr_5Nb_4O_{15}$(s) is calculated to be 600 $J\cdot mol^{-1}\cdot K^{-1}$. The interception of experimental heat capacity values with 3NR values indicate the Debye temperature of the compound. The Debye temperature is calculated to be 750 K for $Sr_5Nb_4O_{15}$(s). The $C_{p,m}$ of $Sr_5Nb_4O_{15}$(s) at 298 K is compared in the Table 4. Table 4 indicates that all values are in good agreement with each other.

Table 4. Heat capacity of $Sr_5Nb_4O_{15}$*(s) at 298 K.*

Compound	$C_{p,m}$ ($J\cdot mol^{-1}\cdot K^{-1}$) at 298 K		
	Own data	Ref.[10]	NKR
$Sr_5Nb_4O_{15}$	477.8	478.5	491.1

3.4. Enthalpy of Formation using High Temperature Oxide Melt Solution Calorimetry

Standard molar enthalpy of formation of $Sr_5Nb_4O_{15}$(s) sample was derived from the enthalpy of dissolution data of the compound and its component oxides viz., SrO(s) and Nb_2O_5(s) in molten $PbO+B_2O_3$ (2:1 molar ratio) solvent maintained at 966 K.

The molar enthalpy of dissolution of SrO(s) was obtained indirectly using a separate thermochemical cycle employing enthalpy of dissolution of its carbonates $SrCO_3$(s).

The details of the experimental measurements have been described elsewhere [13]. For sake of clarity, a schematics of the calorimeter is given in the Figure 6.

Table 5 gives the thermochemical cycle for derivation of standard molar enthalpies of dissolution of SrO(s, 298 K). The enthalpies of decomposition of $\Delta_{decom}H(SrCO_3)$ are -234.3 $kJ\cdot mol^{-1}$. The value of enthalpy increment of CO_2(g) was taken from literature and is equal to 32 $kJ\cdot mol^{-1}$[16].

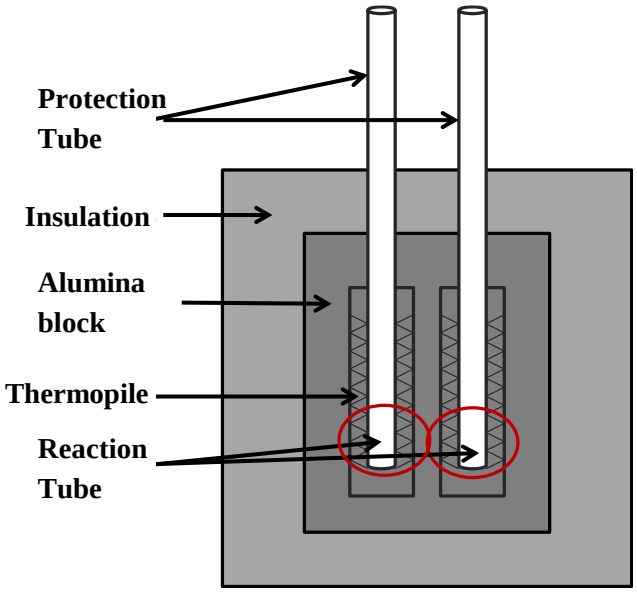

Figure 6. Schematic of high-temperature Calvet-type solution calorimeter (Alexsys-1000, make SETARAM, France).

Table 5. Standard molar enthalpies of dissolution of SrO(s, 298K); sol= molten PbO + B_2O_3 *(2:1) solvent at 966 K;* $\Delta_{ds}H^{o}_{298}(MO)= \Delta H_1 + \Delta H_2 + \Delta H_3$.

Reactions	ΔH_i	Ref.
$SrCO_3$(s, 298 K)+sol(T K)= (SrO)sol(T K) + CO_2(g,T K)	ΔH_1	This Work
SrO(s, 298 K) + CO_2(g, 298 K)= $SrCO_3$ (s, 298 K)	ΔH_2	Ref. [16]
CO_2(g, T K)= CO_2(s, 298 K)	ΔH_3	Ref.[16]
SrO(s, 298 K)+sol(T K) = $(SrO)_{sol}$(T K)	$\Delta_{ds}H^{o}_{298}$	This Work

Enthalpy increments for carbonates are measured at the same experimental temperature and are used for the calculation. The enthalpy of solution of SrO, when added from 298.15 K, $\Delta_{ds}H$(SrO), also known as enthalpy of drop solution, is calculated to be -59.5 $kJ\cdot mol^{-1}$. The enthalpy of solution of the $Sr_5Nb_4O_{15}$(s) in liquid PbO + B_2O_3 (2:1) solvent at 966 K at infinite dilution was measured for few successive additions and presented in Table 6. In our earlier publication, we have reported the enthalpy of solution of Nb_2O_5 in lead borate solvent for the first time and details is given in ref [17]. During each dissolution experiment, the solvent to solute ratio was maintained so that infinite dilution condition is sustained. The values of enthalpies of drop solution of $Sr_5Nb_4O_{15}$(s) from 298 K cited in Table 6, are random in nature which indicates the absence of composition dependence and significant dilution effect.

The enthalpies of drop solution of SrO and Nb_2O_5, obtained in present experiment and other literature data using lead borate solvent are compared in Table 7.

Thermodynamic cycles were constructed to calculate the enthalpy of formation of $Sr_5Nb_4O_{15}$ from the elements and are presented in Table 8.

Table 6: The molar enthalpy of dissolution of $Sr_5Nb_4O_{15}$*(s) in molten* $PbO+B_2O_3$ *(2:1 molar ratio) solvent maintained at 966.1 ± 0.1 K and P =0.1 MPa;* $\Delta_{ds}H_m$ *= molar enthalpy of drop solution.*

Solute	Mass /mg	$\Delta_{ds}H$ /kJ·mol^{-1}
$Sr_5Nb_4O_{15}$ (s)	13.03	323.0
Mol. Mass	13.06	326.1
=1049.72 g·mol^{-1}	13.22	324.3
	14.95	321.9
	17.24	329.8
	14.50	325.5
		Mean: 324.8 ± 3.5

Table 7. Comparison of enthalpy of drop-solution ($\Delta_{ds}H$*) of SrO and* Nb_2O_5 *in lead borate solvent. The error is twice the standard deviation of the mean.*

	$\Delta_{ds}H$/kJ·mol^{-1} in ($2PbO+B_2O_3$) solvent	
	This study	Literature
SrO	-59.5 ± 1.7 at 966 K	-60.5 ± 2.0 at 975 K [21]
Nb_2O_5	66.6± 1.9 at 966 K	-

Table 8. Thermodynamic cycles for the standard molar enthalpy of formation ($\Delta_fH^o_m$ *at 298 K) of* $Sr_5Nb_4O_{15}$ *(s) from elements.*

Reactions	ΔH (kJ·mol^{-1})
$Sr_5Nb_4O_{15}$ (s, 298 K) → 5SrO (dis, 966 K) + $2Nb_2O_5$ (dis, 966 K)	ΔH_1=324(±5)
SrO (s, 298 K) → SrO (dis, 966 K)	ΔH_2 = -58(±2)
Nb_2O_5 (s, 298 K) → Nb_2O_5 (dis, 966 K)	ΔH_3= 68(±2)
Sr (s, 298 K) + 0.5O_2 (g, 298 K) → SrO (s, 298 K)	ΔH_4= -592(±1)[a]
2Nb (s, 298 K) + 2.5O_2 (g, 298 K) → Nb_2O_5 (s, 298 K)	ΔH_5= -1899(±2)[a]
5Sr (298 K) + 4Nb (298 K) + 7.5O_2 (298 K) → $Sr_5Nb_4O_{15}$ (s,298 K)	$\Delta_fH^0_m$(298 K)
Hence, $\Delta_fH^0_m$(298 K) = – ΔH_1 + 5 ΔH_2 + 2ΔH_3 + 5ΔH_4 + 2ΔH_5	**-7236(±7)**

The $\Delta_fH^0_m$(298.15 K) of the compound from the elements is -7236±7 kJ·mol^{-1}. Enthalpy of formation of the component oxides, SrO(s) and Nb_2O_5(s) are taken from ref. [16]. The Gibbs energy of formation was calculated using our enthalpy of formation and entropy of formation at 298 K.

$$\Delta_fG^0_{298}(Sr_5Nb_4O_{15}(s)) = \Delta_fH^0_{298} - 298\times0.001\times\Delta_fS^0_{298} = -6808.4 \text{ kJ·mol}^{-1} \quad (14)$$

The standard molar enthalpy of formation of $Sr_5Nb_4O_{15}$(s) with respect to the constituent oxides (i.e., SrO and Nb_2O_5) at 298 K is found to -478 kJ·mol^{-1}. This indicates that $Sr_5Nb_4O_{15}$ (s) is relatively more stable compared to its binary oxides.

4. Thermal Function of the $Sr_5Nb_4O_{15}$ Compound

The basic function such as $C^o_{p,m}(T)$, $\{H^o_m(T) - H^o_m(298.15\text{ K})\}$ and $\{S^o_m(T) - S^o_m(298.15\text{ K})\}$ as a function of temperature are incorporated in the thermodynamic table as shown in Table 9. The smoothed values of measured heat capacity at regular interval of temperature were used to estimate the standard molar entropy and enthalpy for $Sr_5Nb_4O_{15}$(s). The standard molar entropy and enthalpy for $Sr_5Nb_4O_{15}$ (s) are related to heat capacity as per the relation (15) and (16) respectively.

$$S^0_{TK}(Sr_5Nb_4O_{15}) - S^0_{298\text{ K}}(Sr_5Nb_4O_{15}) = \int^{TK}_{298K}(C_p{}^0(Sr_5Nb_4O_{15})/T)\,dT \quad (15)$$

$$\Delta H^0_{TK}(Sr_5Nb_4O_{15}) - \Delta H^0_{298\text{ K}}(Sr_5Nb_4O_{15}) = \int^{TK}_{298K} C_p{}^0(Sr_5Nb_4O_{15})\,dT \quad (16)$$

The calculated values of these thermodynamic functions have been presented in Table 9 and have an uncertainty of within ±2–3%. The gradual increase of values of the entropy and enthalpy with temperature, indicate the absence of any magnetic and phase transition of the compound. The standard molar entropy of $Sr_5Nb_4O_{15}$(s) was taken from the literature [16]. Free energy function (Fef) for compound can be derived using the following Eq. (16):

$$Fef = -[(H^0_T - H^0_{298})/T] + S^0_T \quad (17)$$

The Free energy function (Fef) of the compound also listed in Table 9 as a function of temperature. Uncertainties for thermodynamic functions were calculated as twice the standard deviation (±2σ) of the experimental values.

Table 9. Thermodynamic functions for the compound $Sr_5Nb_4O_{15}$*(s).*

T/K	*Fitted* C^o_p /J·K^{-1}·mol^{-1}	$(H^o_T - H^o_{298.15})$ /kJ·mol^{-1}	$(S^o_T - S^o_{298.15})$ /J·K^{-1}·mol^{-1}	*Fef* /J·K^{-1}·mol^{-1}
298	477.7	0	0	524.50
300	478.9	1.0	3.19	524.22
400	521.9	56.3	147.45	531.15
500	549.6	116.4	267.06	558.67
600	571.2	180.4	369.23	593.02
700	589.9	247.8	458.71	629.15
800	607.1	318.5	538.62	665.01
900	623.4	392.3	611.08	699.75
1000	639.2	469.1	677.58	733.04

5. Conclusions

Standard enthalpy of formation of $Sr_5Nb_4O_{15}$(s) is determined employing oxide melt solution calorimeter for the first time and is found to be -7236 ± 8 kJ·mol^{-1}. The enthalpy of formation calculated at 965 K from mass spectrometric is found to be -7075 kJ·mol-1. Both the values are in good agreement with each other. The molar heat capacity of the $Sr_5Nb_4O_{15}$(s) is measured using DSC. The standard molar heat capacity of $Sr_5Nb_4O_{15}$(s) derived from the DSC experiment are compared with the values reported by ref.[12]. Smoothed heat capacities values are used for the calculation of the thermodynamic table. The values of standard thermodynamic functions for $Sr_5Nb_4O_{15}$ at T = 298 K are: $C^o_{p,m}$(298 K) = 477.7 J·K^{-1}·mol^{-1}; $\Delta_fH^o_m$(298 K) = -7236 kJ·mol^{-1}; $\Delta_fG^o_m$ (298 K) = - 6808 kJ·mol^{-1}; *fef* (298 K) = 524.5 J·K^{-1}·mol^{-1}. Therefore, this data are important for assessment of fission product interactions and for modeling of fuel thermodynamics which plays an important role in predicting long term stability of these materials under different reactive conditions. Enthalpy of formation and Gibbs energy formation data for this compound would be

useful for predicting the stability of the compound in different physico-chemical conditions.

Nomenclature

$\Delta_f G^o_m$	Molar Gibbs Energy of formation (kJ·mol^{-1})
$\Delta_f H^0_m$	Molar Enthalpy of formation (kJ·mol^{-1})
$\Delta_{ds}H$	Molar Enthalpy of dissolution (kJ·mol^{-1})
$\{H^o_m(T)$-$H^o_m(298$ K)}	Enthalpy Increment (kJ·mol^{-1})
Fef	Free energy function (J·K^{-1}·mol^{-1})
$C^o_{p,m}$	Molar heat capacity at constant pressure (J·K^{-1}·mol^{-1})
M	Molar mass (g·mol^{-1})
T	Temperature (K)
S	Entropy (J·K^{-1}·mol^{-1})
P	Pressure (Pa)
$\Delta_r H^\circ$	Enthalpy of reaction (kJ·mol^{-1})
K_{inst}	Instrumental Constant
I_i^+	Ion current in ampere
σ_i	Electron impact ionization cross-section
a_i	Isotopic abundance of the specific ion.
p_i	Partial pressure

References

[1] F. Galasso, L. Katz, "Preparation and Structure of $Ba_5Ta_4O_{15}$ and Related Compounds," *Acta. Cryst., 14,* 647-651, 1961.

[2] H. Sreemoolanadhan, J. Lsaac, S. Solomon, M.T. Sebastian, K.A. Jose, P. Mohanan, "Dielectric Properties of $Ba_5Nb_4O_{15}$ Ceramic," *Phys. Status Solidi., 143*, 45-49, 1995.

[3] H. Sreemoolanadhan, M.T. Sebastian, P. Mohanan, "High Permittivity and Low Loss Ceramics in the BaO-SrO-Nb_2O_5 System," *Mater. Res. Bull., 30,* 653-658, 1995.

[4] G. Zhu, Z. Ci, C. Ma, Y. Shi, Y. Wang, "A Novel Red Emitting Phosphor of Eu^{3+} Doped TTB-type Niobate $NaSr_2Nb_5O_{15}$ for White Leds,". *Mater. Res. Bull*., *48*, 1995–1998, 2013.

[5] Y. Miseki, H. Kato, A. Kudo, "Water Splitting into H_2 and O_2 over Niobate and Titanate Photocatalysts with (111) Plane-type Layered Perovskite Structure," *Energy Environ. Sci., 2*, 306–314, 2009.

[6] C.D. Whiston, A.J. Smith, Double Oxides Containing Niobium or Tantalum. II. Systems involving Strontium or Barium; *Acta. Cryst. 23*, 82-85, 1967.

[7] M. Weiden, A. Grauel, J. Norwig, S. Horn, F. Steglich, "Crystalline Structure of the Strontium Niobates $Sr_4Nb_2O_9$ and $Sr_5Nb_4O_{15}$," *J. Alloy Compd., 218,* 13-16, 1995.

[8] "The Materials Project. Materials Data on $Sr_5Nb_4O_{15}$," by Materials Project. United States: N. p., 2020. Web. doi:10.17188/1291746.

[9] I.N. Jawahar, P. Mohanan, M.T. Sebastian, "$A_5B_4O_{15}$ (A=Ba, Sr, Mg, Ca, Zn; B=Nb, Ta) microwave dielectric ceramics," *Mater. Lett., 57,* 4043-4048, 2003.

[10] J. R. Carruthers and M. Grasso, "Phase Equilibria Relations in the Ternary System BaO- SrO- Nb_2O_5;" *J. Electrochem. Soc., 117*, 1426-1430, 1970.

[11] Y. Yang, Yu H Jin, "Thermodynamic Calculation of the SrO-Nb_2O_5 System," *J. Mater. Sci. Technol., 15,* 203-207, 1999.

[12] J. Leitner, I. Sipula, K. Ruzica, D. Sedmidubsky, P. Svoboda, "Heat Capacity, Enthalpy and Entropy of Strontium Niobates $Sr_2Nb_{10}O_{27}$ and $Sr_5Nb_4O_{15}$;" *J. Alloys Compd., 481,* 35-39, 2009.

[13] S.K. Rakshit, S.C. Parida, Kristina Lilova, Alexandra Navrotsky, "Thermodynamic studies of $CaLaFe_{11}O_{19}$(s)," *J. Solid State Chem., 20,* 68-74, 2013.

[14] T.D. Mark and E. Hille, "Cross section for single and double ionization of carbon dioxide by electron impact from threshold up to 180 eV;" *J. Chem. Phys., 69*, 2492-2498, 1978.

[15] G.W.H. Hohne, W.F. Hemminger, H.J. Flammershein, (2003), "Differential Scanning Calorimetry," second ed., Springer, Berlin.

[16] Barin I., (1995), "Thermochemical Data of Pure Substances," vol. I & II, 3rd ed., VCH Publishers, New York,.

[17] P. Samui, B.M. Singh, H.V. Khadilkar, S.K. Rakshit, S.C. Parida; "Thermodynamic Studies on $Ba_3SrNb_2O_9$ Employing Calorimeter," *Int. J. Thermodyn., 24,* 50-55, 2021.

[18] M.W. Chase Jr., "JANAF thermochemical tables," fourth ed, Monograph no. 9, J. Phys. Chem. Ref. Data 311-480, 1995.

[19] PCPDFWIN Version 2.2, Joint Committee on Powder Diffraction Standards, JCPDS XRD file No. 00-048-0421.

[20] J. Leitner, M. Nevriva, D. Sedmidubsky, P. Vonka, "Enthalpy of formation of selected mixed oxides in a CaO–SrO–Bi_2O_3–Nb_2O_5 system," *J. Alloy Compd., 509,* 4940-4943, 2011.

[21] B. Joseph, A. Navrotsky, D. Joseph, "Energetics of $La_{2-x}Sr_xCuO_{4-x}$ Solid Solutions ($0.0 < x < 1.0$)," *J. Solid State Chem., 93,* 418-429, 1991.